Self-organization phenomena and decaying self-similar state in two-dimensional incompressible viscous fluids

Yoshiomi Kondoh,* Shunsuke Serizawa, Akihiro Nakano, Toshiki Takahashi, and James W. Van Dam†
Department of Electronic Engineering, Gunma University, Kiryu, Gunma 376-8515, Japan
(Received 12 December 2003; revised manuscript received 23 September 2004; published 28 December 2004)

The final self-similar state of decaying two-dimensional (2D) turbulence in 2D incompressible viscous flow is analytically and numerically investigated for the case with periodic boundaries. It is proved by theoretical analysis and simulations that the sinh-Poisson state $c\omega=-\sinh(\beta\psi)$ is not realized in the dynamical system of interest. It is shown by an eigenfunction spectrum analysis that a sufficient explanation for the self-organization to the decaying self-similar state is the faster energy decay of higher eigenmodes and the energy accumulation to the lowest eigenmode for given boundary conditions due to simultaneous normal and inverse cascading by nonlinear mode couplings. The theoretical prediction is demonstrated to be correct by simulations leading to the lowest eigenmode of $\{(1,0)+(0,1)\}$ of the dissipative operator for the periodic boundaries. It is also clarified that an important process during nonlinear self-organization is an interchange between the dominant operators, which leads to the final decaying self-similar state.

DOI: 10.1103/PhysRevE.70.066312 PACS number(s): 47.27.−i, 05.65.+b, 52.35.Mw, 52.35.Ra

I. INTRODUCTION

The problem of determining the decaying self-similar state in the dynamics of the two-dimensional (2D) incompressible viscous fluid has been addressed for the last decade and is still controversial [1–10]. The general self-organization theories in [7–10] have a common mathematical structure to find the decaying self-similar states as those states for which the rate of change of global autocorrelations for multiple dynamical field quantities is minimized. On the other hand, Taylor published his famous self-organization theory [11] to derive the Taylor state $\nabla\times\mathbf{B}=\lambda\mathbf{B}$ and to explain the appearance of the reversed field pinch configuration in fusion plasma experiments [12], using a conjecture that the magnetic energy is supposed to be minimized by its selective decay compared to the decay of the global magnetic helicity. However, the Taylor state itself had been previously derived from another theory [13] to find the state with minimum dissipation of magnetic energy. The mathematical procedure to find this state is equivalent to that of the selective decay theory, i.e., the global autocorrelation of current density is supposed to be minimized by its selective decay compared to the decay of the global magnetic energy under the assumption of uniform resistivity profile. An interesting fact is that applying the general self-organization theory in [7,8] to the global autocorrelations for the magnetic field under the same assumption of the uniform resistivity profile, we come to a mathematical procedure to find the state with a minimum dissipation of magnetic energy, the same as that of the theory in [13]. This general theory can, however, be applicable to the more general case with nonuniform resistivity, as was demonstrated in [14] by showing agreement between analytical and simulation results for the non-Taylor state. We cannot deal with this general case by using the theory in [13] and Taylor's selective theory [11].

The approach by the selective decay theories was reviewed in [15], based on either a variational principle or an energy principle, and has been discussed in 2D hydrodynamics [1,2]. It should be emphasized here, however, that the Taylor [11] and the selective decay theories are not based on either a variational principle (e.g., as in classical mechanics [16]) or an energy principle (e.g., to describe perturbations in an ideal MHD plasma [17]), but are simply standing on the variational calculus because the two principles lead to dynamical equations for the time evolution of the system of interest. In the case of the 2D incompressible viscous fluid, the selective decay theory was at first applied to lead to a decaying self-similar state with minimal Ω/E (enstrophy/energy) [1,2]. We are able to get this state by applying the general self-organization theory to the fluid velocity, the same as the state with minimum dissipation of magnetic energy in the theory of [13] shown above, as will be clarified in Sec. II. This fact indicates that the general theory [7–10] is a unifying theory for apparently two different theories in [13] and [1,2].

In [4,5], they changed their dominant opinion on the decaying self-similar state from the selective decay theory to the statistical theory by supposing the maximum entropy condition and derived the sinh-Poisson state. It should be noted here, however, that the sinh-Poisson state can never be realized as the decaying self-similar state in the 2D incompressible viscous fluid, as will be analytically clarified in Sec. II.

An alternate approach by the scaling theory was proposed recently, suggesting that the end state is the ultimate stage of a self-similar evolution governing the decay phase [3,6]. As the largest structures are formed, the system eventually ceases to evolve or evolves in a low-dimensional dynamical space [3].

On the other hand, applying the general self-organization theory to the 2D incompressible viscous flow in a friction-

*Email address: kondohy@el.gunma-u.ac.jp
†On leave from Institute for Fusion Studies, The University of Texas at Austin, Austin, Texas 78712, USA.

free box [18] and to the Korteweg–de Vries equation with a dissipative viscosity ν term [19], we clarified by analytical and simulation results that the state with the minimum change rate of the global autocorrelation becomes the decaying self-similar state.

In this paper, since the sinh-Poisson state seems to be widely believed as the decaying self-similar state, analytical proofs and numerical demonstrations are presented to investigate whether the beliefs are true or not. In order to investigate numerically the decaying self-similar state, we need to perform simulations for quite long effective computation times, compared to the simulation data in [4] more than 10 times longer.

In Sec. II, we present a brief description of the general self-organization theory for application to the 2D incompressible viscous fluid, a derivation of the analytical solution for the decaying self-similar state, and relating discussion. We present typical demonstrative results of simulations and discussion in Sec. III, in order to show that the sinh-Poisson state is not realized in the 2D incompressible viscous fluid. Section IV provides a summary.

II. GENERAL THEORY OF SELF-ORGANIZATION AND APPLICATION

A. General theory of self-organization

After we briefly present a general theory extended from [9,10] and originated from [7,8] for how to judge and identify self-organized states in a dissipative nonlinear dynamical system expressed by a general nonlinear set of N simultaneous equations, we will show the application of the general theory to the 2D incompressible viscous flow with periodic boundary conditions. It should be emphasized that the general theory, which uses auto-correlations for dynamical quantities, is not based on either a variational principle or an energy principle, and also that the global auto-correlations are not time invariants.

In order to deal with arbitrary dissipative dynamical systems, we need to develop an abstract type of theory, as follows. Consider a set of N dynamical variables $\mathbf{q} \equiv \mathbf{q}[\xi^k] \equiv (q_1[\xi^k], \ldots, q_N[\xi^k])$, with M-dimensional independent variables $[\xi^k]$ $(k=1,2,\ldots,M)$, which may include time, space, and velocity in distribution functions, or prices, amount of materials, budgets for production systems, and other such variables. Using generalized symbolic dynamical operators, we may write the general nonlinear set of N simultaneous equations for an open or closed dynamical system as

$$\partial q_i[\xi^k]/\partial \xi^j = D_i^j[\mathbf{q}], \tag{1}$$

where ξ^j is one fixed independent variable among $[\xi^k]$, such as time $R_1 t_R$, and $D_i^j[\mathbf{q}]$ $(i=1,2,\ldots,N)$ represents dynamical operators that include both nonlinear and dissipative terms for the change of a dynamical variable q_i along the fixed independent variable ξ^j. In general, however, ξ^j can be any fixed independent variable other than time t, and the dynamical system of interest evolves along ξ^j under Eq. (1). We must note here that the dynamical system of interest always has fluctuations of the dynamical variables $q_i[\xi^k]$ along the axis of the variable ξ^j. The fluctuations may have several characteristic lengths in different orders along ξ^j, one of which is expressed as τ_{ci}. The characteristic length τ_{ci} may give the ordering of the relaxation time scale.

Since the self-organized states must have the most unchangeable configurations along ξ^j during the evolution of the dynamical system, we find that the best algorithm to judge and identify the self-organized states in a dissipative nonlinear dynamical system is by means of the autocorrelation between dynamical variables $q_i[\xi^j]$ and $q_i[\xi^j + (\Delta\xi^j/\tau_{ci})]$, where the increase of ξ^j for q_i is normalized by τ_{ci}. Therefore, we will be able to judge and identify the self-organized states as those states for which the rate of change of global autocorrelations for multiple dynamical field quantities is minimized, that are exactly written by

$$\min \left| \frac{\int q_i[\xi^j] q_i[\xi^j + (\Delta\xi^j/\tau_{ci})] |J_{k\neq j}| \prod_{k\neq j} d\xi^k}{\int (q_i[\xi^k])^2 |J_{k\neq j}| \prod_{k\neq j} d\xi^k} - 1 \right|, \tag{2}$$

where $J_{k\neq j}$ is the Jacobian to yield the well-defined integral for the independent variables $[\xi^k]$ $(k\neq j)$. When we use the variational calculus in the following equations, we do not need any clear expressions of $J_{k\neq j}$. This is because the variational calculus is so constituted that the Jacobian itself does not give any mathematical change to the process of variational calculations. Here, the minimization in Eq. (2) is performed with respect to the dynamical variables $q_i[\xi^k]$ $(i=1,2,\ldots,N)$. Expanding Eq. (2), we obtain the following equivalent criterion for self-organized states to first order in $\Delta\xi^j/\tau_{ci}$:

$$\min \left| \frac{\int q_i[\xi^k](\partial q_i[\xi^k]/\partial \xi^j) |J_{k\neq j}| \prod_{k\neq j} d\xi^k}{\tau_{ci} \int (q_i[\xi^k])^2 |J_{k\neq j}| \prod_{k\neq j} d\xi^k} \right|. \tag{3}$$

Substituting the original dynamical equations of Eq. (1) into Eq. (3), we obtain the final criterion for self-organized states

$$\min \left| \frac{\int q_i[\xi^k] D_i^j[\mathbf{q}] |J_{k\neq j}| \prod_{k\neq j} d\xi^k}{\tau_{ci} \int (q_i[\xi^k])^2 |J_{k\neq j}| \prod_{k\neq j} d\xi^k} \right|. \tag{4}$$

Note that all of the dynamical laws, characterized by the nonlinear simultaneous system of Eq. (1), are embedded in the equivalent criterion of Eq. (4). Since the nonlinear set of N simultaneous equations [Eq. (1)] mutually relate the set of N dynamical variables $q_i[\xi^k]$ $(i=1,2,\ldots,N)$, the mathematical expressions of Eqs. (3) and (4) are obtained by variational calculus with the use of the two functionals F given below, with Lagrange multipliers λ_i

$$F = \int \sum_i \left\{ q_i[\xi^k] \frac{\partial q_i[\xi^k]}{\partial \xi^j} + \tau_{ci} \lambda_i q_i[\xi^k]^2 \right\} |J_{k\neq j}| \prod_{k\neq j} d\xi^k, \tag{5}$$

$$F = \int \sum_i \{ q_i[\xi^k] D_i^j[\mathbf{q}] + \tau_{ci} \lambda_i q_i[\xi^k]^2 \} |J_{k\neq j}| \prod_{k\neq j} d\xi^k. \tag{6}$$

Using $\delta F = 0$ and $\delta^2 F \geqslant 0$, we obtain from Eq. (6) the following Euler-Lagrange equation and its associated eigenvalue equation

$$D_i^{j\#}[\mathbf{q}] + \tau_{ci} \lambda_i q_i^{j\#}[\xi^k] = 0, \tag{7}$$

$$D_i^{j\#}[u] + \tau_{ci} \Lambda_{im} U_{im}[\xi_{k\neq j}^k] = 0. \tag{8}$$

Here, $U_{im}[\xi_{k\neq j}^k]$ is the normalized eigenvalue solutions, and Λ_{im} is the eigenvalue, with the appropriate normalizations written as $\int U_{im}[\xi_{k\neq j}^k] U_{in}[\xi_{k\neq j}^k] |J_{k\neq j}| \Pi_{k\neq j} d\xi^k = \delta_{mn}$, as has been earlier reported [7,8]. Using the second variations of Eq. (6) [9,10], we obtain the following condition for the self-organized state with the minimum rate of change:

$$0 < \lambda_i \leqslant \lambda_{i1}, \tag{9}$$

where λ_{i1} is the smallest positive eigenvalue and λ_i is taken to be positive.

Since we have the normalized eigenvalue solutions $U_{im}[\xi_{k\neq j}^k]$, the profile for each dynamical variable $q_i[\xi_{k\neq j}^k]$ can be expanded at each instance with respect to the variable ξ^j, as follows:

$$q_i[\xi_{k\neq j}^k] = \sum_{m=1}^{\infty} C_{im} U_{im}[\xi_{k\neq j}^k]. \tag{10}$$

Substituting Eq. (10) into Eq. (1), we get the spectrum transfer equations involving the nonlinear dissipative operators $D_i^{j\#}[U]$

$$\sum_{m=1}^{\infty} \frac{\partial C_{im}}{\partial \xi^j} U_{im}[\xi_{k\neq j}^k] = D_i^j[(\sum_{m=1}^{\infty} C_{1m} U_{im}[\xi_{k\neq j}^k], \ldots, \sum_{m=1}^{\infty} C_{Nm} U_{im}[\xi_{k\neq j}^k])]. \tag{11}$$

Since the normalized eigenvalue solutions $U_{im}[\xi_{k\neq j}^k]$ satisfy Eq. (8), the operators $D_i^{j\#}[U]$ will induce nonlinear mode coupling $(\Lambda_{im} \pm \Lambda_{in})$ both to higher and to lower eigenmodes, i.e., simultaneous normal and inverse cascades. Thus, Eq. (11) shows a physical picture for the process of self-organization in the following way: (i) Simultaneous normal and inverse cascadings take place to accompany the more rapid energy decay in the higher eigenmodes. (ii) Consequently, spectrum energy accumulates in the lowest eigenmode that is allowed for given boundary conditions and becomes self-organized and self-similar decaying states $U_{i1}[\xi_{k\neq j}^k]$ $(i = 1, 2, \ldots, N)$.

In the same way that Eq. (7) was derived from the first and the second variations of Eq. (6), we obtain the Euler-Lagrange equation from Eq. (5) as follows:

$$\frac{\partial q_i^{j\#}[\xi^k]}{\partial \xi^j} + \tau_{ci} \lambda_i q_i^{j\#}[\xi^k] = 0. \tag{12}$$

Combining Eqs. (7), (8), and (12) and taking account of the eigenmode spectrum analysis, we obtain the final equations for the self-organized states

$$\frac{\partial q_i^{j\#}[\xi^k]}{\partial \xi^j} = D_i^{j\#}[\mathbf{U}] = -\tau_{ci} \Lambda_{i1} U_{i1}[\xi_{k\neq j}^k]. \tag{13}$$

These self-organized states must satisfy the original Eq. (1) and the boundary conditions. Equation (13) yields the final solutions for the self-similar, slowest decay phase with the smallest eigenvalue Λ_{i1}

$$q_i^{j\#}[\xi^k] = \exp(-\tau_{ci} \Lambda_{i1} \xi^j) U_{i1}[\xi_{k\neq j}^k]. \tag{14}$$

The final analytic solutions, Eq. (14), definitely shows that the self-organized state is not "the stationary state," but is "the decaying self-similar state" with the slowest speed within characteristic decay time τ_{ci}, because of the dissipative feature of the dynamical system of interest. This theoretical result is consistent with the physical picture for the process of self-organization that we found with the use of eigenmode spectrum analysis, as was discussed at Eq. (11).

B. Application to the 2D incompressible viscous fluid

We apply the general theory shown above to the 2D incompressible viscous fluid with periodic boundary conditions in the x,y plane (normalized to unit length). Taking the curl of the Navier-Stokes equation, we use the following vorticity representation

$$\frac{\partial \boldsymbol{\omega}}{\partial t} = -(\mathbf{u} \cdot \boldsymbol{\nabla}) \boldsymbol{\omega} + \nu \nabla^2 \boldsymbol{\omega}. \tag{15}$$

Here, $\mathbf{u}(x,y)$ is the fluid velocity, $\boldsymbol{\omega}(x,y) = \boldsymbol{\nabla} \times \mathbf{u}$ is the vorticity, ν is the kinematic viscosity, and $\boldsymbol{\nabla} \cdot \mathbf{u} = 0$. In dimensionless units, the kinematic viscosity ν is the reciprocal of the Reynolds number R for unit length and unit initial rms velocity, i.e., $\nu = R^{-1}$. Multiplying R to Eq. (15), and normalizing time axis by R, we get a vorticity equation with the normalized time by the Reynolds number as follows:

$$\frac{\partial \boldsymbol{\omega}}{\partial t_R} = -R(\mathbf{u} \cdot \boldsymbol{\nabla}) \boldsymbol{\omega} + \nabla^2 \boldsymbol{\omega}, \tag{16}$$

where $t_R \equiv t/R$. The nondissipative and dissipative operators correspond to the $-R(\mathbf{u} \cdot \boldsymbol{\nabla}) \boldsymbol{\omega}$ term and the $\nabla^2 \boldsymbol{\omega}$ term in Eq. (16), respectively.

Using the periodic boundary conditions for Eq. (16), we obtain the following functional F corresponding to Eq. (6) in the general theory

$$F = \int_x \int_y [\boldsymbol{\omega} \cdot (-\boldsymbol{\nabla} \times \boldsymbol{\nabla} \times \boldsymbol{\omega} + \tau_{ci} \lambda \boldsymbol{\omega})] dx dy. \tag{17}$$

Since the effective dissipative operator $D_i^j[\mathbf{q}]$ is given by $-\boldsymbol{\nabla} \times \boldsymbol{\nabla} \times \boldsymbol{\omega}$ in Eq. (17), we directly obtain the Euler-Lagrange equation from Eq. (7), which corresponds to Eq. (8), for the self-organized state $\boldsymbol{\omega}^{\#}$ reported in [8] as follows:

$$\nabla \times \nabla \times \boldsymbol{\omega}^{\#} = \Lambda \boldsymbol{\omega}^{\#}. \tag{18}$$

The value of τ_{ci} is taken to be unity, since the self-organized state of a 2D incompressible viscous fluid has negligibly small fluctuations. If we work in the velocity representation of the Navier-Stokes equation, we obtain the same type of Euler-Lagrange equation for the velocity $\mathbf{u}^{\#}$ at this self-organized state [7,8], namely,

$$\nabla \times \nabla \times \mathbf{u}^{\#} = \Lambda \mathbf{u}^{\#}. \tag{19}$$

We can rewrite the Euler-Lagrange equations for $\boldsymbol{\omega}^{\#}$ and $\mathbf{u}^{\#}$ as $\nabla^2 \boldsymbol{\omega}^{\#} = -\Lambda \boldsymbol{\omega}^{\#}$ and $\nabla^2 \mathbf{u}^{\#} = -\Lambda \mathbf{u}^{\#}$.

Corresponding to Eq. (8) in the general theory, we obtain the following eigenvalue equations [7,8]:

$$\nabla \times \nabla \times \boldsymbol{\omega}_k^{\#} - \Lambda_k \boldsymbol{\omega}_k^{\#} = 0, \tag{20}$$

$$\nabla \times \nabla \times \mathbf{u}_k^{\#} - \Lambda_k \mathbf{u}_k^{\#} = 0, \tag{21}$$

where Λ_k is the eigenvalue, and $\boldsymbol{\omega}_k^{\#}$ and $\mathbf{u}_k^{\#}$ denote the eigensolutions.

On the other hand, owing to the self-adjoint property of the present dissipative operator [7,8], the eigenfunctions $\mathbf{a}_k$ for the associated eigenvalue problems form a complete orthogonal set and the appropriate normalization is written as

$$\int \mathbf{a}_k \cdot (\nabla \times \nabla \times \mathbf{a}_j) dV = \int \mathbf{a}_j \cdot (\nabla \times \nabla \times \mathbf{a}_k) dV = \Lambda_k \int \mathbf{a}_j \cdot \mathbf{a}_k dV = \Lambda_k \delta_{jk}, \tag{22}$$

where $\nabla \times \nabla \times \mathbf{a}_k - \Lambda_k \mathbf{a}_k = 0$ is used. For the present case with the periodic boundary conditions in the x,y plane (normalized to unit length), the normalized orthogonal eigenfunctions $\mathbf{a}_{\omega k}$ for the vorticity and $\mathbf{a}_{uk}$ for the velocity are obtained, respectively, as follows:

$$\mathbf{a}_{\omega k} = \exp[i2\pi(l_k x + m_k y)]\mathbf{k}, \tag{23}$$

$$\mathbf{a}_{uk} = \frac{1}{\sqrt{l_k^2 + m_k^2}} \exp[i2\pi(l_k x + m_k y)](-m_k \mathbf{i} + l_k \mathbf{j}), \tag{24}$$

where $\Lambda_k = 4\pi^2(l_k^2 + m_k^2)$, $l_k \geqslant 0, m_k \geqslant 0$, except for $l_k = 0$ and $m_k = 0$ at the same time. Here, $\nabla \times \mathbf{a}_{uk} = i2\pi\sqrt{l_k^2 + m_k^2}\,\mathbf{a}_{\omega k}$. Using Λ_1^2 of the lowest $\{(1,0)+(0,1)\}$ mode for this case with the periodic boundaries, we obtain $\Lambda_1 = 4\pi^2$.

The profiles for $\boldsymbol{\omega}$ and $\mathbf{u}$ at each instance can be expanded, respectively, by $\mathbf{a}_{\omega k}$ and $\mathbf{a}_{uk}$ as follows:

$$\boldsymbol{\omega} = \sum_{k=-\infty}^{\infty} C_{\omega k} \mathbf{a}_{\omega k}, \tag{25}$$

$$\mathbf{u} = \sum_{k=-\infty}^{\infty} C_{uk} \mathbf{a}_{uk}, \tag{26}$$

where the spectra of $C_{\omega k}$ and C_{uk} $(k = 1,2,\ldots)$ depend now on time $R_1 t_R$. Substituting Eqs. (23)–(26) into Eq. (16), we obtain the following spectrum transfer equation, corresponding to Eq. (11) in the general theory

$$\sum_{k=\infty}^{\infty} \frac{\partial C_{\omega k}}{\partial t_R} \exp[i2\pi(l_k x + m_k y)]\mathbf{k} = \sum_{k=\infty}^{\infty} \sum_{j=0}^{\infty} \left(-i2\pi R C_{\omega k} C_{uj} \frac{\mp l_k m_j \pm l_j m_k}{\sqrt{l_k^2 + m_k^2}} \times \exp\{i2\pi[(l_k \pm l_j)x + (m_k \pm m_j)y]\}\mathbf{k} + C_{\omega k} 4\pi(l_k^2 + m_k^2) \times \exp\{[i2\pi(l_k x + m_k y)]\}\mathbf{k} \right). \tag{27}$$

It can be seen from Eq. (27) that if the flow system contains multiple eigenmodes (l_j, m_j) with $j = 1, 2, 3, \ldots$, the larger Reynolds number in the first term of right-hand side [deduced from the nonlinear term $-R(\mathbf{u} \cdot \nabla)\omega$] induces the faster spectrum transfers in the present time scale of t_R to both the higher and the lower eigenmodes of $(l_k \pm l_j, m_k \pm m_j)$ by mode couplings, i.e., by simultaneous normal and inverse cascadings [18]. At the same time, the second term [deduced from the dissipative term $\nabla^2 \boldsymbol{\omega}$] yields the higher dissipation for the higher eigenmodes proportionally to the square of the mode numbers $l_k^2 + m_k^2$. Therefore, collaborating with the dissipative term, the nonlinear term works to accumulate flow energies at the lowest eigenmode which persists to the end [18]. It is important to note that any single eigenmode solution satisfies the equation $-R(\mathbf{u} \cdot \nabla)\omega = 0$ for the nonlinear term of Eq. (16). In other words, any single eigenmode solution can become one of the self-similar states of decaying 2D turbulence. Then, the lowest eigenmode, which is persisted to the end as discussed above with use of Eq. (27), never induces further different eigenmodes and, therefore, becomes the final self-organized state for the decaying 2D turbulence. These analytical results will be demonstrated by simulations in Sec. III.

Since the fluid velocity is given by $\mathbf{u} = \nabla \psi \times \mathbf{k}$ with the use of the stream function $\psi = \psi(x,y,t)$, which is independent of z as are all other field variables, the equation between ω and ψ is given by

$$\nabla^2 \psi = -\omega. \tag{28}$$

Using the lowest eigensolution of Eq. (23), we can obtain the relation between ω and ψ as follows:

$$\omega = 4\pi^2 \psi. \tag{29}$$

In the case of the scaling theory, the end state is suggested to be the ultimate state of a self-similar evolution governing the decay phase [3,6]. This indicates that since the self-organized and decaying self-similar state, denoted by superscript of #, must have an essential feature to keep its profile and to decay its amplitude self-similarly, the state to be derived from Eq. (16) must analytically satisfy "the condition of the self-similar decay" written as

$$\frac{\partial \boldsymbol{\omega}^{\#}}{\partial t_R} = -R(\mathbf{u}^{\#} \cdot \nabla)\omega^{\#} + \nabla^2 \boldsymbol{\omega}^{\#} = -\alpha\, \boldsymbol{\omega}^{\#}. \tag{30}$$

If the state of interest satisfies this condition, the state is proved to be the decaying self-similar state, but not to be the stationary state. In the case of statistical theory [4,5], how-

ever, the derived sinh-Poisson state $c\omega=-\sinh(\beta\psi)$ always fulfills $-R(\mathbf{u}^{\#}\cdot\boldsymbol{\nabla})\omega^{\#}=0$, but it is not the solution for $\nabla^2\boldsymbol{\omega}^{\#}=-\alpha\,\boldsymbol{\omega}^{\#}$. Therefore, the sinh-Poisson state can never satisfy the condition of the self-similar decay even for any large Reynolds numbers R, and it cannot analytically become the decaying self-similar state. If we neglect the dissipative term $\boldsymbol{\nabla}^2\boldsymbol{\omega}$, we can easily find that the sinh-Poisson state is an analytical solution for $\partial\boldsymbol{\omega}/\partial t_R=-R(\mathbf{u}\cdot\boldsymbol{\nabla})\omega=0$, i.e., the sinh-Poisson state is the stationary state itself. However, if we use other initial multivortex distributions and numerically solve the equation $\partial\boldsymbol{\omega}/\partial t_R=-R(\mathbf{u}\cdot\boldsymbol{\nabla})\omega$, then we can never obtain the sinh-Poisson state itself and also the decaying self-similar state without numerical error, such as the numerical diffusion. This fact definitely means that the sinh-Poisson state never appears in any accurate numerical simulations. If the sinh-Poisson state is realized with the use of some simulations, then those results become a clear proof that those simulations contain serious numerical errors. The nonappearance of the sinh-Poisson state in the dynamical evolution of the 2D incompressible viscous fluid belongs to an essential problem that this state can never become an analytical solution for the two original Eqs. (15) and (16) and Eq. (30) required for the decaying self-similar state.

On the other hand, the lowest eigenmode solution of Eqs. (23) and (24) satisfies Eq. (30) as follows:

$$\frac{\partial\boldsymbol{\omega}_1^{\#}}{\partial t_R}=-R(\mathbf{u}_1^{\#}\cdot\boldsymbol{\nabla})\omega_1^{\#}+\boldsymbol{\nabla}^2\boldsymbol{\omega}_1^{\#}=-\Lambda_1\boldsymbol{\omega}_1^{\#}. \tag{31}$$

Equation (31) yields the final solutions of the self-similar and slowest decay state with the smallest eigenvalue Λ_1 written by

$$\begin{aligned}\boldsymbol{\omega}^{\#}(t_R,x,y)&=\exp(-\Lambda_1 t_R)\mathbf{a}_{\omega 1}\\&=\exp(-4\pi^2 t_R)[\cos 2\pi x+\cos 2\pi y]\mathbf{k},\end{aligned} \tag{32}$$

where $\Lambda_1=4\pi^2$ of the lowest $\{(1,0)+(0,1)\}$ mode is used. Equations (31) and (32) are the analytical results predicted by the general theory to find self-organized states written at Eqs. (13) and (14). It is seen from Eq. (32) that the decay constant of the self-organized state is determined by the lowest eigenvalue $\Lambda_1=4\pi^2$, and it does not depend on the Reynolds number R in the present time scale of t_R.

We now derive minimal Ω/E (enstrophy/energy) based on the selective theory [1,2], using Eq. (3) of the general self-organization theory. Putting $q_i[\xi^k]=\mathbf{u}(x,y),\xi^j=t_R$ and $\tau_{ci}=1$, we obtain the condition to find the decaying self-similar and self-organized state from Eq. (3) as

$$\min\left|\frac{(\partial/\partial t_R)\int_x\int_y(\mathbf{u}\cdot\mathbf{u})\mathrm{d}x\mathrm{d}y}{2\int_x\int_y(\mathbf{u}\cdot\mathbf{u})\mathrm{d}x\mathrm{d}y}\right|. \tag{33}$$

Repesenting energy E and enstropy Ω as $E\equiv\int_x\int_y(\mathbf{u}\cdot\mathbf{u})\mathrm{d}x\mathrm{d}y$ and $\Omega\equiv\int_x\int_y(\omega\cdot\omega)\mathrm{d}x\mathrm{d}y$, respectively, and using Eq. (16), vector formulas, the Gauss theorem, and the periodic boudary conditions, we obtain the following:

$$\frac{\partial E}{\partial t_R}=-\frac{2}{\rho}\int_x\int_y(\omega\cdot\omega)\mathrm{d}x\mathrm{d}y=-\frac{2}{\rho}\Omega. \tag{34}$$

Substituting Eq. (34) into Eq. (33), we obtain exactly the same condition with minimal Ω/E based on the selective theory [1,2] to derive the decaying self-similar and self-organized state, as follows:

$$\min\frac{1}{\rho}\frac{\Omega}{E}. \tag{35}$$

Since initial distributions with a large number of small size random vortexes were used in [1,2], and they stopped their computation at an earlier time in their simulations, they could not reach the exact decaying self-similar state as shown by the analytical solution Eq. (32). In the same way as shown above, the theory of minimum dissipation of magnetic energy in [13] can be derived by setting $q_i[\xi^k]=\mathbf{B}$ and using relation of $(\partial/\partial t)\int_V(\mathbf{B}\cdot\mathbf{B})\mathrm{d}V=2\mu_0\int_V(\eta\mathbf{j}\cdot\mathbf{j})\mathrm{d}V$ with the use of Ohm's law with resistivity η, as follows:

$$\min\left|\frac{\mu_0\int_V(\eta\mathbf{j}\cdot\mathbf{j})\mathrm{d}V}{\int_V(\mathbf{B}\cdot\mathbf{B})\mathrm{d}V}\right|. \tag{36}$$

If we assume uniform resistivity to lead to the Taylor state, we see that Eq. (36) becomes identical to the theory in [13], but we can find the non-Taylor state for nonuniform resistivity, as was analytically and numerically demonstrated in [14]. We can recognize from two derivations shown above that the general theory [7–10] is a unifying theory for apparently two different theories in [13] and [1,2], which are applied to different physical objects.

In order to investigate the correlation between the analytical equations for the self-organized states and the simulation data, we will calculate numerically the correlation coefficient $C(f,g)$ between two functions f and g, which is defined as follows:

$$C(f,g)=\frac{\overline{(f-\overline{f})(g-\overline{g})}}{[\overline{(f-\overline{f})^2}\,\overline{(g-\overline{g})^2}]^{1/2}}. \tag{37}$$

We will show later how the correlation coefficient between simulation data and this relation of $\omega=4\pi^2\psi$ becomes close to unity as the final self-organized state appears in time.

We consider here the ratio between the nonlinear coupling term and the dissipative term. We treat the root-mean-square average of the nonlinear coupling term and that of dissipative term, respectively, as

$$N_d = \frac{1}{l^2}\sqrt{\int_0^1\int_0^1 \{R(\mathbf{u}\cdot\boldsymbol{\nabla})\boldsymbol{\omega}\}^2 \mathrm{d}x\mathrm{d}y}, \tag{38}$$

$$D_d = \frac{1}{l^2}\sqrt{\int_0^1\int_0^1 (\nabla^2\boldsymbol{\omega})^2 \mathrm{d}x\mathrm{d}y}, \tag{39}$$

where l is boundary length with edge length 1. In order to investigate the dominantly working operator, we introduce two quantities of D and N, defined by $D=D_d/(D_d+N_d)$ and $N=N_d/(D_d+N_d)$, respectively. We call here D and N as "the dissipative ratio" and "the nondissipative ratio," respectively. When the nonlinear coupling term is dominant compared to the dissipative term, then $D \ll N$. When the self-similar state is realized in the free-decaying 2D turbulence, the state comes to satisfy the equation $-R(\mathbf{u}\cdot\boldsymbol{\nabla})\omega=0$, and, hence, N_d goes to zero. Therefore, it is seen from expressions of N and D that $D\sim 1$ and $N\sim 0$ at the self-similar state. The dominant operator changes, consequently, from the nonlinear term to the dissipative term in the free-decaying 2D turbulence. This interchange of dominant operator will be shown later in the following numerical simulations.

III. COMPUTATIONAL RESULTS AND DISCUSSION

We solve Eq. (16) in a dimensionless unit, under the conditions of periodic boundaries in x,y plane (normalized to unit length). The initial distributions of the present simulations are given by superposition of several eigenmodes for the eigensolutions of Eq. (23). The hyperbolic equation of Eq. (16) is solved with the use of a different type scheme, named the KOND (kernel optimum nearly analytical discretization algorithm) scheme [20,21], which has high numerical accuracy and stability. We use the JACOBI scheme [22] to solve the elliptic type equation $\nabla^2\psi=-\omega$. Numerical procedures at each time step are as follows: (i) solve $\nabla^2\psi=-\omega$ by the JACOBI scheme to get values of ψ, (ii) get values of $\mathbf{u}$ from ψ, (iii) solve Eq. (16) by the KOND scheme to get values of $\boldsymbol{\omega}$, and (iv) go to (i) for the next time step. The simulation domain is implemented on a $[(5+101+5)\times(5+101+5)]$ point grid with the grid interval of 0.01 in the x and y directions. It should be emphasized that, because the initial large size vortex distributions with only several eigenmodes are used here, the number of grid points shown above is sufficient to get correct time evolutions of the present fluid dynamics by using the KOND [20,21] and the JACOBI schemes [22], both of which have high numerical accuracy and stability. On the other hand, because initial distributions with a large number of small size random vortexes are used in [1,2,4,5], they have to use a large number of grid points, such as $[(4096)\times(4096)]$, for their simulations, and this large number of grid points itself prevents them from investigating simulations for very long computation times, for example, more than 10 times longer, compared to the simulations in [4]. The periodic conditions are applied at the boundaries of the inside domain of (101×101) point grids, and the extra layers with five-point grids surrounding the inside domain are used to sweep out numerically diffusive errors that occur from the outermost edges of the simulation domain. In order to eliminate the numerical errors that propagate inward in the extra layers, all data in the extra layers are replaced by the corresponding data on the grids in the inside domain before the numerical errors reach at the boundary of the inside domain. The time step is basically set as $\Delta t=0.0001$. In order to suppress the appearance of numerical errors, however, when the maximum values of $\partial\omega/\partial x$ and $\partial\omega/\partial y$ become 10 times greater than their average values, the time step is reduced to be one order smaller as $\Delta t=0.00001$.

In this paper, we show typical data of simulations with two cases of $R=R_1\equiv 1400$ and $R=R_2\equiv 14\,000$. In figures of simulation data, we use a common time axis with $R_1 t_R$ in order to compare the two cases under the same equivalent normalized time. We show typical results of simulations for the initial flow, which is given by superposition of four eigenmodes of (1, 3), (1, 4), $-(3,1)$, and $-(4,1)$, with the use of Eq. (24) for the velocity. Here, $-(3,1)$ and $-(4,1)$ mean that their amplitudes are multiplied by minus. The initial flow contains the same amount of positive and negative eigenmode components of vorticities. It should be emphasized here that the initial flow does not contain the lowest eigenmodes of $\{(1,0)+(0,1)\}$ that is analytically predicted for the slowest decaying self-similar state given by Eq. (32).

First, we compare the typical time evolutions of the vorticity structure for the two cases of $R=R_1$ and $R=R_2$, which are respectively shown in Figs. 1 and 2. In those figures, the bold and the broken lines show contour plots of positive vorticity and those of negative one, respectively. The height of the contours is normalized by the maximum absolute value of either the positive or negative vorticity in each figure. In earlier phases around $R_1 t_R=0.5$ in Fig. 1 and around $R_1 t_R=0.1$ in Fig. 2, the nonlinear process changes the initial vorticity structure into the more complicated one with small-scale deformations, and the like-sign vortex capture takes place as was reported in [1–6,18]. At $R_1 t_R=4.5$ in Fig. 1 and at $R_1 t_R=0.4$ in Fig. 2, there appear positive and negative vorticities that are relatively steep and isolated from each other. These features were also observed in other simulations reported in [3], where they propose the scaling theory, and in [5], where they propose the statistical theory. As time goes on, we find that the simplest structure with the lowest eigenmodes of $\{(1,0)+(0,1)\}$ remains to become the decaying self-similar state, as is shown in the contour plots at $R_1 t_R=50$ in both Figs. 1 and 2. This decaying self-similar structure was also reported in [1], where the selective decay theory is suggested.

It is recognized from the comparison between the two cases of Figs. 1 and 2 that since the nonlinear term $-R(\mathbf{u}\cdot\nabla)\boldsymbol{\omega}$ in Eq. (16) written by the normalized time scale is 10 times larger for the latter case as compared to the former one, the nonlinear process changes the vorticity structure almost 10 times faster in the latter case than in the former one, while the slowest decaying self-similar state appears at almost the same normalized time.

Figures 3 and 4 show the typical time evolutions of the spectral components of vorticity during the self-organization process of the flow structure, which are obtained from the simulation data shown in Figs. 1 and 2, respectively. In those

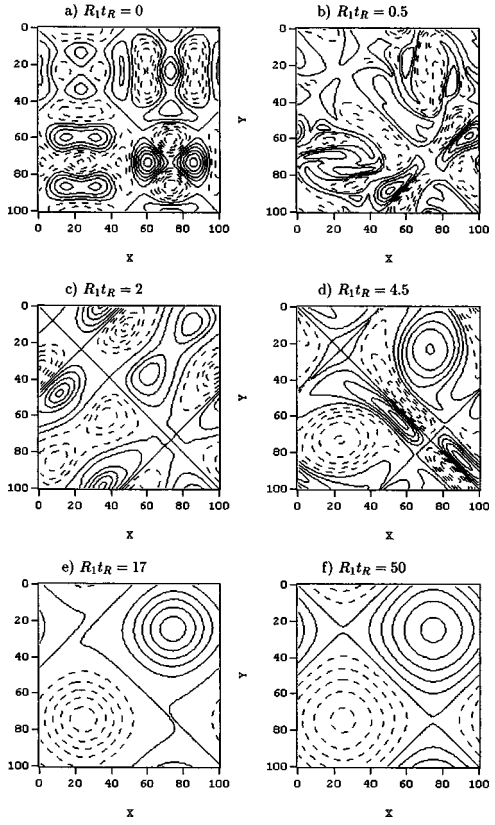

FIG. 1. Typical time evolution of vorticity structure during self-organization for the case of $R=1400$.

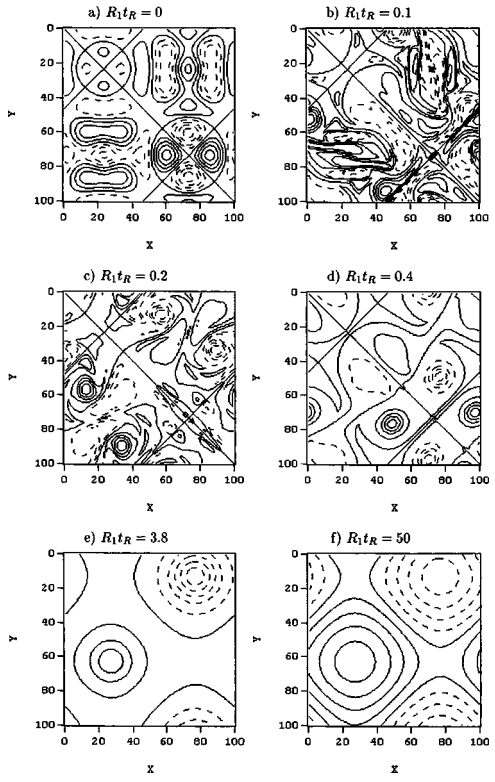

FIG. 2. Time evolution of vorticity structure during self-organization for the case of $R=14000$.

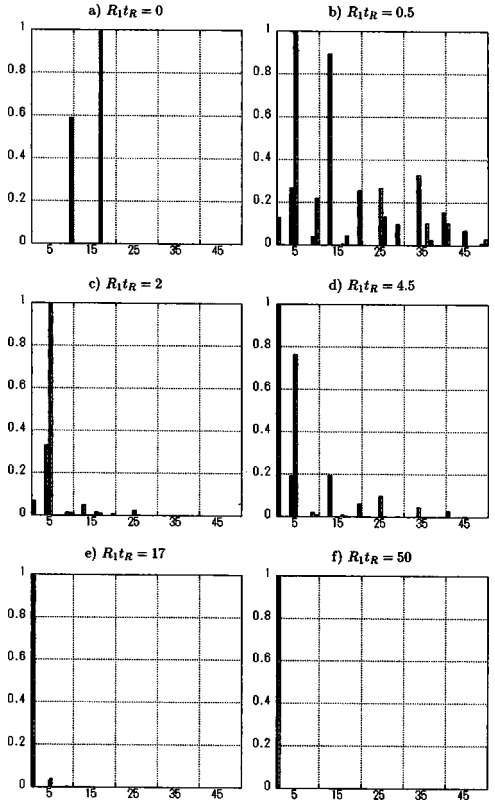

FIG. 3. Time evolution of spectral components of vorticity for the case of $R=1400$.

figures, the horizontal scale is given by the spectral eigenvalues $\Lambda_k=\pi^2(l_k^2+m_k^2)$ for eigenmodes (l_k,m_k). The vertical scale is normalized by the maximum absolute value of either the positive or the negative spectral components $C_{\omega k}$ in each figure, where the positive spectra are shown by bold bars and the negative ones by shaded bars attached to the right-hand side of the bold bars. The initial spectra for the four eigenmodes of (1,3), (1,4), $-(3,1)$, and $-(4,1)$ are seen to be shown only by the two positive and the two negative lines in both figures at $R_1t_R=0$. We find from the spectrum in earlier phases at $R_1t_R=0.5$ in Fig. 3 and at $R_1t_R=0.1$ in Fig. 4 that the nonlinear process yields the spectrum transfer toward both the higher and the lower spectral eigenmodes, in other words, it yields that the wave number flows toward both the smaller side (the inverse cascade) and to the larger one (the normal cascade) on the wave number space. It is seen from the time evolution of spectra after the earlier phases that the higher spectral components dissipate more rapidly and the inverse cascade yields, gradually, spectrum accumulation at the lowest eigenmodes of $\{(1,0)+(0,1)\}$, which remains to become the decaying self-similar state, as is shown by the spectrum at $R_1t_R=50$ in Figs. 3 and 4. The amplitude of (1,0) mode is equal to that of (0,1) mode at $R_1t_R=50$. We should note here that the eigenmodes of $\{(1,0)+(0,1)\}$ were not contained in the initial flow at $R_1t_R=0$, but have been induced nonlinearly during the self-organization process.

It is clearly seen again from the comparison between the two cases of Figs. 3 and 4 that the 10-times-larger nonlinear term $-R(\mathbf{u}\cdot\nabla)\boldsymbol{\omega}$ in the latter case yields the almost 10-

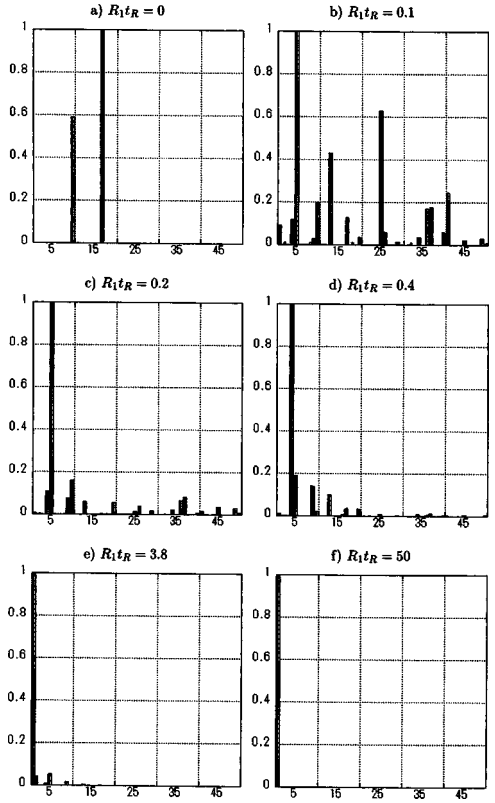

FIG. 4. Time evolution of spectral components of vorticity for the case of $R=14000$.

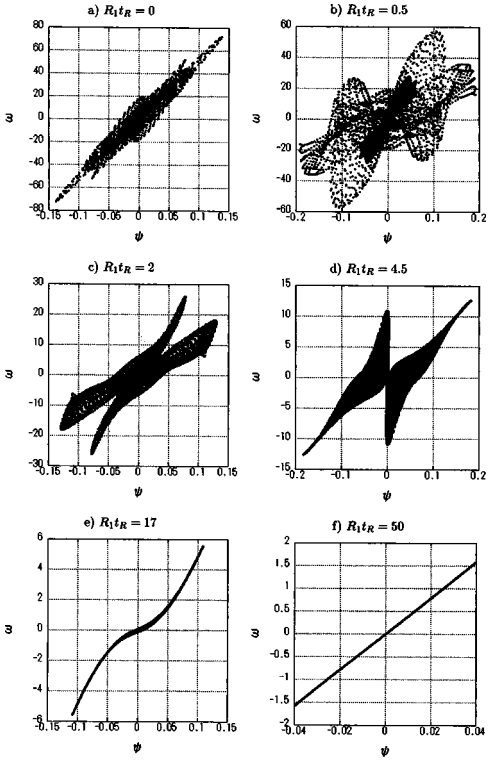

FIG. 5. Time evolution of the relation between ω and ψ for the case of $R=1400$.

times-faster spectrum transfer toward both the higher and lower spectral eigenmodes than in the former case, resulting in similarly faster dissipation of the higher spectral components by the dissipative term $\nabla^2\boldsymbol{\omega}$ in Eq. (16) and in faster spectrum accumulation at the lowest eigenmodes of $\{(1,0)+(0,1)\}$, consequently, in the present normalized time scale.

Figures 5 and 6 show the typical time evolutions of the relation between ω and ψ during the self-organization process for the simulation data shown in Figs. 1 and 2, respectively. The horizontal scale is ψ, and the vertical scale is ω. Since normal and inverse cascades occur in earlier phases at around $R_1t_R=0.5$ in Fig. 3 and at around $R_1t_R=0.1$ in Fig. 4, the data of ω and ψ exhibit a complicated distribution on the $\omega-\psi$ plane at the corresponding time in Figs. 5 and 6. After the earlier phases, corresponding to the rapid dissipation of higher spectral components and the gradual spectrum accumulation to the lowest eigenmodes of $\{(1,0)+(0,1)\}$, the scattered data begin to concentrate and show clearer structures. At $R_1t_R=17$ in Fig. 5 and at $R_1t_R=3.8$ in Fig. 6, the concentrated data become curves, which are, on the whole, similar to those of the sinh-Poisson state $\omega=c\sinh(\beta\psi)$. However, when we go on to calculate further, the data on the $\omega-\psi$ plane clearly come to the straight line given by $\omega=4\pi^2\psi$ at $R_1t_R=50$ in both Figs. 5 and 6, as was predicted analytically at Eq. (29).

Figures 7 and 8 show the time evolutions of dominant operators $D=D_d/(D_d+N_d)$ and $N=N_d/(D_d+N_d)$ during the self-organization process, which are obtained from the simulation data shown in Figs. 1 and 2, respectively, with the use of Eqs. (38) and (39). It is seen from Figs. 7 and 8 that the nonlinear terms are dominant in earlier phases in both figures and the dominant operators are exchanged from the nonlinear terms to the dissipative ones at around $R_1t_R=17$ in Fig. 7 and at around $R_1t_R=3$ in Fig. 8. It is clear, however, that after the exchange of the dominant operators, the nonlinear terms in both figures decrease rapidly to be negligibly small compared to the dissipative ones in the present normalized time scale. We may understand from Figs. 7 and 8 the reason why the nonlinear term $-R(\mathbf{u}\cdot\nabla)\boldsymbol{\omega}$ comes to have no power to determine the final ordered structure of the present two-dimensional incompressible viscous fluids: the physical feature that the nonlinear term yields completely the seat of the dominant operator to the dissipative one after a certain time on the time scale normalized by R, even if R is quite large.

Figures 9 and 10 show, respectively, the time evolutions of the correlation coefficients between the simulation data of Figs. 1 and 2 with our analytical relation of $\omega=4\pi^2\psi$ and those with $\omega=c\sinh(\beta\psi)$ of the sinh-Poisson state. In those figures, the bold line is the correlation coefficient for $\omega=4\pi^2\psi$ and the chain-dotted line is for $\omega=c\sinh(\beta\psi)$. It is seen from the chain-dotted line in those figures that even though the values of the correlation coefficients for $\omega=c\sinh(\beta\psi)$ come close to unity at around $R_1t_R=13$ in Fig. 9 and at around $R_1t_R=3$ in Fig. 10, respectively, they never become 1.0 and deviate fairly fast away to be lower than those for $\omega=4\pi^2\psi$ at $R_1t_R=20$ in Fig. 9 and at $R_1t_R=10$ in Fig. 10, respectively. Those results definitely mean that the sinh-Poisson state never becomes the solution for the original Eq. (16), as was analytically proved after Eq. (30). On the other hand, the values of the correlation coefficients for

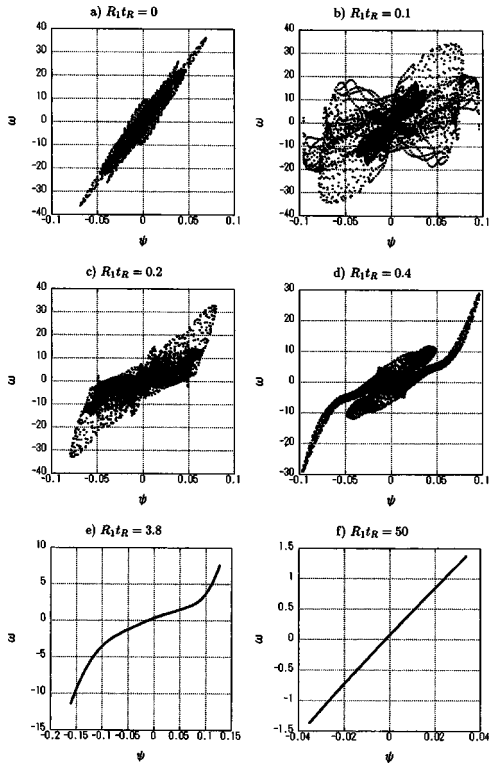

FIG. 6. Time evolution of the relation between ω and ψ for the case of $R=14000$.

$\omega=4\pi^2\psi$ become almost completely united after around $R_1t_R=28$ in Fig. 9 and after around $R_1t_R=25$ in Fig. 10, respectively.

It should be noted here that, by referring to Figs. 1–4 and 7–10, the decaying self-similar state has already established at around $R_1t_R=25$–28 in the normalized time scale, and the structure of the vortex does not change, but only the vortex amplitude decreases gradually with time after the realization of the decaying self-similar and self-organized state.

We find from comparison of Fig. 9 and Fig. 10 that when we replot data along the present time scale normalized by the Reynolds number R, then the establishment time τ_e of the decaying self-similar state becomes almost the same time as mentioned above, whose value of time depends on initial vortex distributions. In the normalized time scale, we see from Figs. 9 and 10 that the larger value of R yields the earlier appearance and the faster disappearance of a state, which is not exactly the same but is similar to the sinh-Poisson state. The nonappearance of the sinh-Poisson state in the dynamical evolution of the 2D incompressible viscous fluid is analytically proved after Eq. (30), by showing that this state does not become an analytical solution for the original Eq. (16).

IV. SUMMARY

In Sec. II A, we presented the general theory, extended from [9,10] and originated from [7,8], for how to judge and identify self-organized states in general dissipative nonlinear dynamical systems from the view point of observations and

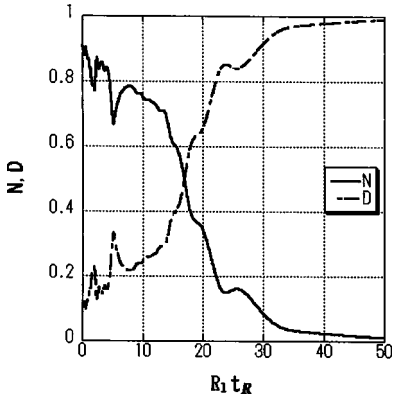

FIG. 7. Time evolutions of dominant operators $D=D_d/(D_d+N_d)$ and $N=N_d/(D_d+N_d)$ for the case of $R=1400$.

applied it to the 2D incompressible viscous fluid in Sec. II B to obtain the decaying self-similar solution Eq. (32) deduced from Eq. (31) and satisfying the original Eq. (16) written in the time scale normalized by the Reynolds number R. The two Eqs. (31) and (32) are directly connected with the general analytical results of Eqs. (13) and (14) deduced from the general theory. Applying the eigenfunction spectrum analysis to the 2D turbulent process with the use of the normalized orthogonal eigenfunctions Eqs. (23) and (24), we deduced the following physical picture, which is independent with values of R to explain sufficiently the self-organization with two simple and fundamental mechanisms: (i) Simultaneous normal and inverse cascading by nonlinear mode couplings. (ii) The faster spectral decay of higher eigenmodes and the spectral accumulation to the lowest eigenmode for given boundary conditions. We also derived the analytical relation between the vorticity and the stream function written as $\omega=4\pi^2\psi$ for the decaying self-similar state. We analytically proved that the sinh-Poisson state never appears in the dynamical evolution of the 2D incompressible viscous fluid by showing that this state never becomes the analytical solution for both of the original Eq. (16) and Eq. (30) required for "the decaying self-similar state."

We analytically showed that the general theory [7–10] is a unifying theory for apparently different two theories of minimum dissipation of magnetic energy in [13] and of minimal

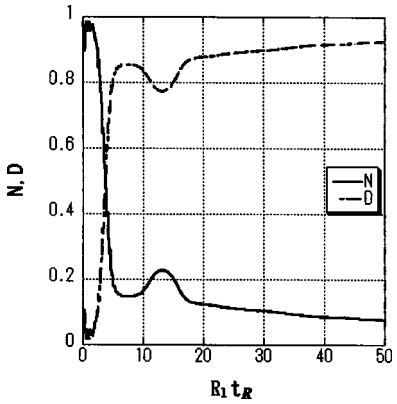

FIG. 8. Time evolutions of dominant operators $D=D_d/(D_d+N_d)$ and $N=N_d/(D_d+N_d)$ for the case of $R=14000$.

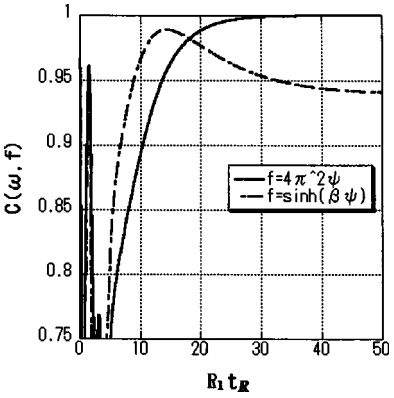

FIG. 9. Time evolutions of the correlation coefficients between the simulation data of Fig. 1 with $\omega=4\pi^2\psi$ and those with $\omega=c\sinh(\beta\psi)$. $R=1400$.

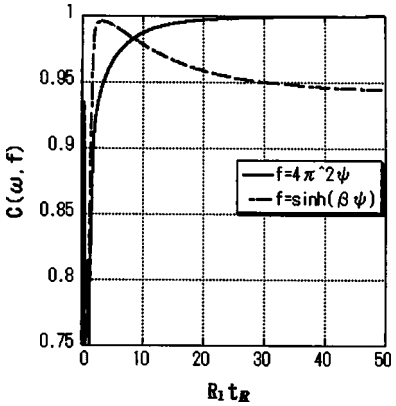

FIG. 10. Time evolutions of the correlation coefficients between the simulation data of Fig. 2 with $\omega=4\pi^2\psi$ and those with $\omega=c\sinh(\beta\psi)$. $R=14000$.

Ω/E (enstrophy/energy) based on the selective theory in [1,2].

In Sec. III, the theoretical prediction together with the physical picture of self-organization to the decaying self-similar state was demonstrated to be correct by simulations that exactly realize the theoretical solution of the lowest eigenmode $\{(1,0)+(0,1)\}$ for the case of the periodic boundaries. It is also clarified that an important process during nonlinear self-organization is the interchange of the dominant operators, through which there appears the decaying self-similar state with the lowest eigenmode of the dissipative operator (cf. Figs. 7 and 8). Showing that the value of the correlation coefficient for the sinh-Poisson state with simulation data never becomes 1.0 in Figs. 9 and 10, we have clarified that this state never becomes the solution for the original Eq. (16), as was analytically proved after Eq. (30). On the other hand, these two figures show that the value of the correlation coefficient for $\omega=4\pi^2\psi$ becomes almost completely 1.0 at almost the same time around $R_1t_R=25$–28 in the normalized time scale, as was analytically predicted at Eq. (31). It is, however, worthwhile to note that before the interchange of the dominant operators, there appear transitional states similar to the sinh-Poisson state on the whole.

The most remarkable feature of the present general theory to be emphasized is that it can be applicable not only to the turbulent 2D incompressible viscous fluid, but also to any dissipative nonlinear dynamical systems [written by Eq. (1)], giving decaying self-similar and self-organized states as the Euler-Lagrange equations.

ACKNOWLEDGMENTS

The authors would like to thank Dr. N. Kondo, M. Yamaguchi, T. Fukasawa, and Y. Inatani for their valuable discussion and help on programing for our spectrum analysis. This work was carried out under the collaborative research program at the NIFS, Toki, and was supported by a Grant-in Aid for Scientific Research from the Ministry of Education, Science and Culture, Japan.

[1] W. H. Matthaeus, W. T. Stribling, D. Martinez, S. Oughton, and D. Montgomery, Physica D **51**, 531 (1991).
[2] W. H. Matthaeus, W. T. Stribling, D. Martinez, S. Oughton, and D. Montgomery, Phys. Rev. Lett. **66**, 2731 (1991).
[3] G. F. Carnevale, J. C. McWilliams, Y. Pomeau, J. B. Weiss, and W. R. Young, Phys. Fluids A **4**, 1314 (1992).
[4] D. Montgomery, W. H. Matthaeus, W. T. Stribling, D. Martinez, and S. Oughton, Phys. Fluids A **4**, 3 (1992).
[5] D. Montgomery, X. Shan, and W. H. Matthaeus, Phys. Fluids A **5**, 2207 (1993).
[6] D. Marteau, O. Cardoso, and P. Tabeling, Phys. Rev. E **51**, 5124 (1995).
[7] Y. Kondoh, Phys. Rev. E **48**, 2975 (1993).
[8] Y. Kondoh, Phys. Rev. E **49**, 5546 (1994).
[9] Y. Kondoh, T. Takahashi, and J. W. Van Dam, J. Plasma Fusion Res. **5**, 598 (2002).
[10] Y. Kondoh, T. Takahashi, and J. W. Van Dam, Derivation of Non-Invariance of Magnetic Helicity in Ideal Plasmas Surrounded by a Completely Conducting Wall and a General Theory of Self-Organization for Open and Dissipative Dynamical Systems, *Proceedings of Ninth IEA/RFP Workshop, Tsukuba, Japan, 5–7 March 2003* (unpublished).
[11] J. B. Taylor, Phys. Rev. Lett. **33**, 1139 (1974).
[12] H. A. B. Bodin and A. A. Newton, Nucl. Fusion **20**, 1255 (1980).
[13] S. Chandrasekhar and L. Woltijer, Proc. Natl. Acad. Sci. U.S.A. **44**, 285 (1958).
[14] Y. Kondoh, *et al.*, J. Phys. Soc. Jpn. **63**, 546 (1994).
[15] A. Hasegawa, Adv. Phys. **34**, 1 (1985).
[16] H. Goldstein, *Classical Mechanics* (Addison-Wesley, Reading, MA, 1957), Sec. II.
[17] I. B. Bernstein, E. A. Frieman, M. D. Kruskal, and R. M.

Kulsrud, Proc. R. Soc. London, Ser. A **244**, 17 (1958).
[18] Y. Kondoh, M. Yoshizawa, A. Nakano, and T. Yabe, Phys. Rev. E **54**, 3017 (1996).
[19] Y. Kondoh and J. W. Van Dam, Phys. Rev. E **52**, 1721 (1995).
[20] Y. Kondoh, J. Phys. Soc. Jpn. **60**, 2851 (1991).
[21] Y. Kondoh, Y. Hosaka, and K. Ishii, Comput. Math. Appl. **27**, 59 (1994).
[22] M. Salvadori and M. Baron, *Numerical Methods in Engineering* (Prentice-Hall, Englewood Cliffs, NJ, 1961).